Squeezing Via Spontaneous Rotational Symmetry Breaking in a Four-Wave Mixing Cavity

Ferran V. Garcia-Ferrer, Carlos Navarrete-Benlloch, Germán J. de Valcárcel, and Eugenio Roldán

***Abstract*—We predict the generation of noncritically squeezed light through the spontaneous rotational symmetry breaking occurring in a Kerr cavity. The model considers a $\chi^{(3)}$ cavity that is pumped by two Gaussian beams of frequencies ω_1 and ω_2. The cavity configuration is such that two signal modes of equal frequency $\omega_s = (\omega_1 + \omega_2)/2$ are generated, these signal fields being first-order Laguerre–Gauss modes. In this system, a spontaneous breaking of the rotational symmetry occurs as the signal field corresponds to a Hermite–Gauss TEM mode. This symmetry breaking leads to the perfect and noncritical (i.e., nondependent on the parameter values) squeezing of the angular momentum of the output TEM mode, which is another TEM mode spatially orthogonal to that in which bright emission occurs.**

***Index Terms*—Four-wave mixing (FWM), nonlinear optics, quantum fluctuations, squeezed light.**

I. Introduction

SQUEEZED light is a kind of radiation exhibiting reduced fluctuations with respect to vacuum in some special observable. This occurs at the obvious expense of an increase in the fluctuations of its canonical pair, as followed by the Heisenberg uncertainty relation satisfied by the couple. In a single-mode field, these canonically related observables correspond to orthogonal field quadratures, which are equivalent to the position and momentum of a harmonic oscillator. Squeezing is a macroscopic manifestation of quantum phenomena that is attracting continuous attention since the late seventies of the past century [1]–[3]. Nowadays, a renewed interest has arisen because of the importance of squeezing in generating continuous variable entanglement, which is a central issue for continuous variable quantum information purposes [4].

Squeezed light is generated by means of nonlinear optical processes, such as parametric down-conversion or four-wave mixing. The squeezing level attainable in such nonlinear optical processes depends on the interaction time that is limited by the nonlinear medium length. Thus, in order to increase the squeezing level, these processes are usually confined to occur within an optical cavity. In this way, the squeezing level can reach the largest possible levels at the system bifurcation points such as, e.g., the emission threshold. Squeezing levels as large as 90% (10 dB reduction with respect to vacuum fluctuations) have been recently reported [5], [6] under such conditions in degenerate optical parametric oscillators (DOPOs). However, perfect squeezing (i.e., the complete suppression of quantum fluctuations in a field observable) cannot be achieved under these conditions because complete suppression of fluctuations in a mode quadrature implies the existence of infinite fluctuations in the other quadrature, what would require infinite energy in the process.

Nevertheless, perfect squeezing could be actually produced as some of us have recently proposed [7]. The idea can be put in short as follows. Consider a nonlinear optical process in which two photons with equal frequency are generated in Laguerre–Gauss modes with opposite orbital angular momentum (OAM) equal to ± 1. This is equivalent to generating two photons in a TEM_{10} Hermite–Gauss mode whose orientation in the transverse *x*–*y* plane is determined by the relative phase between the two Laguerre–Gauss photons, let us denote it by ϕ. Now, assume that ϕ is not fixed as it occurs, e.g., in a down-conversion process. This amounts to saying that the orientation of the Hermite–Gauss mode is not fixed as ϕ is the angle formed by the Hermite–Gauss mode with respect to the *x*-axis. under these conditions, we can expect the occurrence of unbounded fluctuations in the Hermite–Gauss mode orientation, which suggests that the canonical pair of ϕ, namely the angular momentum $-i\partial/\partial\phi$, can be perfectly fixed. But the angular momentum of a TEM_{10} mode forming an angle ϕ with respect to the *x* axis is another TEM_{10} mode forming an angle $\phi + \pi/2$ with respect to the *x*-axis. Then, this mode could exhibit perfect squeezing in one of its field quadratures. Note that the concept of bifurcation is not involved in this discussion and that the variable exhibiting unbounded fluctuations is an angle. Then, *a priori*, perfect squeezing is possible in such a process as "infinite" fluctuations are possible in the orientation ϕ.

Some of us in [7] and [8] have theoretically demonstrated the earlier ideas in a DOPO tuned to the first transverse mode family at the down-converted frequency. The requirement that the angle ϕ can take any possible value (i.e., that the phase difference between the two Laguerre–Gauss modes be arbitrary) is nothing but the requirement that the system be rotationally invariant around the axis of the optical cavity. Hence, the resulting squeezing can be understood as well as the result of the spontaneous breaking of this rotational symmetry, as the emitted Hermite–Gauss mode is obviously no more rotationally invariant. We extended this study in [9] to DOPOs having different transverse mode families resonating at the down-converted frequency, arriving to the same conclusion: every time the

Manuscript received April 08, 2009; revised July 01, 2009. Current version published November 04, 2009. This work was supported by the Spanish Ministerio de Ciencia e Innovación and the European Union FEDER under Project FIS2005-07931-C03-01 and Project FIS2008-06024-C03-01. The work of C. Navarrete-Benlloch was supported by a grant from the Programa FPU del Ministerio de Ciencia e Innovación.

The authors are with the Department d'Òptica, Universitat de València, 46100 Valencia, Spain (e-mail: ferran.garcia@uv.es; carlos.navarrete@uv.es; german.valcarcel@uv.es; eugenio.roldan@uv.es).

Color versions of one or more of the figures in this paper are available online at http://ieeexplore.ieee.org.

Digital Object Identifier 10.1109/JQE.2009.2028616

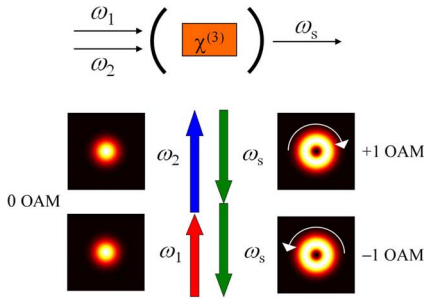

Fig. 1. Scheme of the system. A $\chi^{(3)}$ medium is confined within an optical cavity and pumped by two Gaussian beams of frequencies ω_1 and ω_2. The cavity tuning is such that two signal modes with frequency $\omega_s = (\omega_1 + \omega_2)/2$ are generated. The two signal modes are degenerated in frequency but differ in the spatial mode, one (the other) corresponding to a Laguerre–Gauss mode with $+1$ (-1) OAM.

nonlinear process generates light which breaks the rotational invariance of the system, the expected perfect squeezing is found.

In the present paper, we study a model for a $\chi^{(3)}$-nonlinear cavity in which squeezing appears as the result of the spontaneous rotational symmetry breaking. The interest of this new proposal is twofold. On one hand, it allows us to demonstrate that rotational symmetry breaking is a robust means for generating squeezing in the sense that is not limited to a $\chi^{(2)}$-nonlinear cavity such as the DOPO. On the other hand, perfect rotational invariance could be problematic to achieve in $\chi^{(2)}$ systems because phase-matching requirements can imply the tilting of the nonlinear crystal, thus compromising rotational invariance, a difficulty that disappears in a $\chi^{(3)}$ process because phase-matching occurs easily in this case.

The type of $\chi^{(3)}$-nonlinear cavity system, we are proposing here is a novel one that has not been studied previously, as far as we know. Hence, we derive the quantum model (see Section II) as well as study its classical emission properties (see Section III) before addressing its quantum properties (see Section IV). We are able to demonstrate that the proposed device effectively exhibits perfect squeezing originating in the rotational symmetry breaking. In Section V, we summarize our main results.

II. Model

Consider an optical cavity with spherical mirrors containing an isotropic $\chi^{(3)}$ medium. The cavity is pumped from the outside with two coherent fields of frequencies ω_1 and ω_2, these pumping beams having a Gaussian transverse profile. Suppose, for simplicity, that these pumping beams have the frequencies and shapes corresponding to two consecutive longitudinal modes of the optical cavity. Then, within the cavity the nonlinear interaction generates, through an FWM process, two other fields having the same frequency ω_s such that $\omega_1 + \omega_2 = 2\omega_s$. Assume now that the cavity geometry and tuning is such that these two signal fields have the shape of first-order Laguerre–Gauss modes. These modes carry OAM and its conservation imposes that one of the signal fields carries $+1$ OAM, while the other carries -1 OAM as the pumping fields have zero OAM (see Fig. 1).

As stated, the just described FWM process requires that the optical cavity modes, as well as the fields' frequencies, be properly chosen. An immediate choice that verifies the previous requirements is a symmetric confocal resonator, where the even and odd OAM modes are well separated in frequency (see Appendix A for a short review of the modal structure of a general resonator). This is thus the cavity that we discuss here for simplicity, although we show in Appendix A that nearly symmetric, nearly confocal resonators can be used with equivalent results.

In a confocal, the resonance frequency of longitudinal mode q corresponding to the transverse family $f = 2p + l$ (p is the mode's radial index, while l is the absolute value of its OAM) is given by [10]

$$\omega_{qf} = \frac{\pi c}{L}\left(q + \frac{1+f}{2}\right) \tag{1}$$

where L is the effective cavity length.

In the simplest scheme, the pumping beams of our model can correspond to two consecutive longitudinal modes q and $q+1$ with $f = 0$. The signal modes would then correspond to the cavity modes with indexes q and $f = 1$, as they verify $2\omega_s = \omega_{q,0} + \omega_{q+1,0} = 2\omega_{q,1}$. Certainly, in the confocal resonator there are other modes with frequency ω_s having odd OAM (all the modes belonging to odd families), but we can neglect them by considering that these higher order Laguerre–Gauss modes have smaller coupling with the pump modes (and higher diffraction losses indeed) and would consequently not be amplified [9].

Once we have shown that the FWM process we propose could be experimentally implemented, we pass to formulate the mathematical model of our system.

A. Fields

We shall assume for simplicity that the $\chi^{(3)}$ medium is placed at the cavity's waist plane and that is thin enough as to perform the uniform field approximation, hence neglecting any dependence of the fields on the axial coordinate z. Thus, we write the total quantum field inside the cavity, at the beam waist, as

$$\hat{E}(\mathbf{r},t) = \hat{E}_{\mathrm{p}}(\mathbf{r},t) + \hat{E}_s(\mathbf{r},t) \tag{2a}$$

$$\hat{E}_{\mathrm{p}}(\mathbf{r},t) = \sum_{j=1,2} i\mathcal{F}_j \hat{A}_j(\mathbf{r},t)e^{-i\omega_j t} + \mathrm{H.c.} \tag{2b}$$

$$\hat{E}_s(\mathbf{r},t) = i\mathcal{F}_s \hat{A}_s(\mathbf{r},t)e^{-i\omega_s t} + \mathrm{H.c.} \tag{2c}$$

where H.c. stands for Hermitian conjugate, $\mathbf{r} = r(\cos\phi, \sin\phi)$ is the position vector in the transverse plane written in polar coordinates, subindices p and s denote pump and signal modes, respectively, $\mathcal{F}_k^2 = \hbar\omega_k/(\varepsilon_0 nL)$, with k =1, 2, s, and n is the refractive index (we neglect dispersion for simplicity). The slowly varying envelopes are

$$\hat{A}_j(\mathbf{r},t) = \hat{a}_j(t)G_j(\mathbf{r}), \qquad j = 1,2 \tag{3a}$$

$$\hat{A}_s(\mathbf{r},t) = \hat{a}_+(t)L_+(\mathbf{r}) + \hat{a}_-(t)L_-(\mathbf{r}) \tag{3b}$$

with $\hat{a}_k(t)$ and $\hat{a}_k^\dagger(t)$ the annihilation and creation operators for mode $k = 1,2,+,-$, which verify $[\hat{a}_m(t), \hat{a}_n^\dagger(t)] = \delta_{mn}$. As for the spatial dependence in (3), they are given by [10]

$$G_j(\mathbf{r}) = \sqrt{\frac{2}{\pi}}\frac{1}{w_j}e^{-(r/w_j)^2}, \qquad j = 1,2 \tag{4a}$$

$$L_{\pm 1}(\mathbf{r}) = \frac{2}{\sqrt{\pi}}\frac{r}{w_s^2}e^{-(r/w_s)^2}e^{\pm i\phi} \tag{4b}$$

for the Gaussian and first-order Laguerre–Gauss modes, respectively. In all cases, $w_j \propto 1/\sqrt{\omega_j}$, $j = 1, 2, s$. Note, however, that in the optical domain, in which $\omega_1 \sim 10^{15}\ \mathrm{s}^{-1}$, one can safely take $\omega_1 \simeq \omega_2 \simeq \omega_s$ as far as L is not very small, which implies that the waist is very nearly the same for all of the involved modes. We make this approximation that, although not essential, simplifies some expressions shortly.

For later use, we need the relation between the Laguerre–Gauss modes and the Hermite–Gauss modes

$$H_{10}^{\sigma} = \frac{e^{-i\sigma}L_{+1} + e^{i\sigma}L_{-1}}{\sqrt{2}} = \sqrt{2}\,|L_{\pm 1}(\mathbf{r})|\cos(\phi - \sigma) \quad (5a)$$

$$H_{01}^{\sigma} = \frac{e^{-i\sigma}L_{+1} - e^{i\sigma}L_{-1}}{i\sqrt{2}} = \sqrt{2}\,|L_{\pm 1}(\mathbf{r})|\sin(\phi - \sigma) \quad (5b)$$

with H_{10}^{σ} and H_{01}^{σ} being the Hermite–Gauss modes with an orientation σ and $\sigma + \pi/2$ with respect to the x-axis, respectively. Thus, the slowly varying amplitudes at frequency ω_s can also be written as

$$\hat{A}_s(\mathbf{r}, t) = \hat{a}_{10,\sigma}(t)H_{10}^{\sigma} + \hat{a}_{01,\sigma}(t)H_{01}^{\sigma} \quad (6)$$

with

$$\hat{a}_{10,\sigma} = \frac{1}{\sqrt{2}}(e^{i\sigma}\hat{a}_{+} + e^{-i\sigma}\hat{a}_{-}) \quad (7a)$$

$$\hat{a}_{01,\sigma} = \frac{i}{\sqrt{2}}(e^{i\sigma}\hat{a}_{+} - e^{-i\sigma}\hat{a}_{-}) \quad (7b)$$

the annihilation operators for the Hermite–Gauss modes. Finally, we introduce the field quadratures of these Hermite–Gauss modes

$$\hat{X}_{j,\sigma}^{\varphi} = e^{-i\varphi}\hat{a}_{j,\sigma} + e^{i\varphi}\hat{a}_{j,\sigma}^{\dagger}, \quad j = 10, 01 \quad (8)$$

with $\hat{a}_{10,\sigma}$ and $\hat{a}_{01,\sigma}$ given by (7).

B. Hamiltonian

In the interaction picture, the system's Hamiltonian can be written as

$$\hat{H} = \hat{H}_0 + \hat{H}_{\mathrm{ext}} + \hat{H}_{\mathrm{int}}. \quad (9)$$

where $\hat{H}_0$ and $\hat{H}_{\mathrm{ext}}$ correspond to the modes' energies and external injection, respectively, and are given by

$$\hat{H}_0 = \sum_{j=1,2,+,-} \hbar\delta_j a_j^{\dagger} a_j \quad (10a)$$

$$\hat{H}_{\mathrm{ext}} = i\hbar\mathcal{E}_1\left(\hat{a}_1^{\dagger} - \hat{a}_1\right) + i\hbar\mathcal{E}_2\left(\hat{a}_2^{\dagger} - \hat{a}_2\right) \quad (10b)$$

with $\delta_j = (\omega_{Cj} - \omega_j)$ the cavity detuning for the mode with frequency ω_j, ω_{Cj} being the cavity resonance closest to that mode. In a confocal resonator, this detuning is the same for all the modes if the relative frequency of the pump modes is locked to the free spectral range of the cavity, i.e., $\omega_2 - \omega_1 = \pi c/L$. Hence, in the following we take $\delta_j = \delta\ \forall\ j$. $\mathcal{E}_j$ are the pumping parameters, which are related to the experimental parameters by

$$\mathcal{E}_j = \sqrt{\frac{n\gamma_j}{\hbar\omega_j}P_j} \quad (11)$$

$\gamma_j = cT_j/2L$ being the cavity decay rate at the considered frequency (T_j is the corresponding transmission factor through the input mirror) and P_j the power of the pump laser. In the following, we will assume $\mathcal{E}_1 = \mathcal{E}_2 = \mathcal{E}$ for simplicity. $\hat{H}_{\mathrm{int}}$ describes the nonlinear interaction and can be written as the sum of three contributions

$$\hat{H}_{\mathrm{int}} = -\hbar g(\hat{H}_{\mathrm{spm}} + \hat{H}_{\mathrm{cpm}} + \hat{H}_{\mathrm{fwm}}) \quad (12)$$

with

$$\hat{H}_{\mathrm{spm}} = \hat{a}_1^{\dagger 2}\hat{a}_1^2 + \hat{a}_2^{\dagger 2}\hat{a}_2^2 + \frac{1}{2}\left(\hat{a}_+^{\dagger 2}\hat{a}_+^2 + \hat{a}_-^{\dagger 2}\hat{a}_-^2\right) \quad (13)$$

$$\hat{H}_{\mathrm{cpm}} = 4\hat{a}_1^{\dagger}\hat{a}_1\hat{a}_2^{\dagger}\hat{a}_2 + 2\hat{a}_+^{\dagger}\hat{a}_+\hat{a}_-^{\dagger}\hat{a}_- + 2\left(\hat{a}_1^{\dagger}\hat{a}_1 + \hat{a}_2^{\dagger}\hat{a}_2\right)\left(\hat{a}_+^{\dagger}\hat{a}_+ + \hat{a}_-^{\dagger}\hat{a}_-\right) \quad (14)$$

$$\hat{H}_{\mathrm{fwm}} = 2\left(\hat{a}_1^{\dagger}\hat{a}_2^{\dagger}\hat{a}_+\hat{a}_- + \hat{a}_1\hat{a}_2\hat{a}_+^{\dagger}\hat{a}_-^{\dagger}\right) \quad (15)$$

describing self-phase modulation, cross-phase modulation, and four-wave mixing, respectively. Note that this Hamiltonian contains all the possible combinations of four operators conserving both energy and OAM. The factors multiplying the different terms are intuitive once one takes into account the two following features: 1) there is a global factor 4 in $\hat{H}_{\mathrm{cpm}}$ and $\hat{H}_{\mathrm{fwm}}$ with respect to $\hat{H}_{\mathrm{spm}}$ coming from all possible permutations of the different operators and 2) if any of the four modes is a signal mode, a factor 1/2 appears that comes from the transverse modes' overlapping integral. Finally, it can be shown that the coupling constant is given by

$$g = \frac{6\mathcal{F}^4\varepsilon_0 l_{\mathrm{m}}\chi}{\pi\hbar w^2} \quad (16)$$

with w the beam waist, l_{m} the nonlinear medium length, and χ the relevant third-order nonlinear susceptibility.

C. Quantum Evolution Equations

In this section, we apply the standard procedure to develop the quantum theory of a nonlinear resonator within the generalized P representation to our Kerr cavity model [11]–[13]. The starting point is the system's master equation for the density operator $\hat{\varrho}$, which reads

$$\frac{d}{dt}\hat{\varrho} = \frac{1}{i\hbar}[\hat{H}, \hat{\varrho}] + \widehat{\mathcal{L}\varrho} \quad (17)$$

where $\mathcal{L}$ is the Liouvillian superoperator describing field losses through the output mirror, which applied to the density operator reads

$$\widehat{\mathcal{L}\varrho} = \sum_{j=1,2,+,-} \gamma_j\left(\left[\hat{a}_j, \hat{\varrho}\hat{a}_j^{\dagger}\right] + \left[\hat{a}_j\hat{\varrho}, \hat{a}_j^{\dagger}\right]\right). \quad (18)$$

As we are assuming that the system has perfect rotational symmetry around the cavity axis it follows that $\gamma_+ = \gamma_- \equiv \gamma_s$.

As usual, we use now the generalized P representation in order to transform the operator master equation into a partial differential equation for the quasi-probability distribution P. In this representation, to every pair of boson operators $(\hat{a}_j, \hat{a}_j^{\dagger})$, it corresponds a pair of independent stochastic amplitudes

(α_j, α_j^+) verifying $\langle \alpha_j^+ \rangle = \langle \alpha_j \rangle^*$. By using standard techniques, one finds that the Fokker–Planck equation governing the evolution of P reads

$$\frac{\partial}{\partial t} P(\boldsymbol{\alpha}; t) = \left[-\frac{\partial}{\partial \alpha_i} A_i + \frac{1}{2} \frac{\partial^2}{\partial \alpha_i \partial \alpha_j} \mathcal{D}_{ij} \right] P(\boldsymbol{\alpha}; t) \tag{19}$$

where we write vector $\boldsymbol{\alpha}$ as

$$\boldsymbol{\alpha} = \left(\alpha_1, \alpha_2, \alpha_+, \alpha_-, \alpha_1^+, \alpha_2^+, \alpha_+^+, \alpha_-^+ \right) \tag{20}$$

and give the explicit expression of the components of both the drift vector $\mathbf{A}(\boldsymbol{\alpha})$ and the diffusion matrix $\mathcal{D}(\boldsymbol{\alpha})$ in Appendix B.

Once the Fokker–Planck equation is known, it can be converted, by applying Ito rules, into an equivalent set of stochastic first-order differential equations: the quantum Langevin equations. They read

$$\frac{d}{dt} \boldsymbol{\alpha} = \mathbf{A}(\boldsymbol{\alpha}) + \mathcal{B}(\boldsymbol{\alpha}) \cdot \boldsymbol{\eta}(t) \tag{21}$$

where the components of $\boldsymbol{\eta}(t)$ are real Gaussian noises verifying

$$\langle \eta_i(t) \rangle = 0 \tag{22a}$$

$$\langle \eta_i(t) \eta_j(t') \rangle = \delta_{ij} \delta(t - t') \tag{22b}$$

and the noise matrix $\mathcal{B}$ can be obtained from

$$\mathcal{D} = \mathcal{B} \cdot \mathcal{B}^T. \tag{23}$$

The equivalency between the master equation and Langevin equations must be understood as follows:

$$\left\langle : f\left(\hat{a}_m, \hat{a}_m^\dagger \right) : \right\rangle = \left\langle f\left(\alpha_m, \alpha_m^+ \right) \right\rangle_{\text{stochastic}} \tag{24}$$

i.e., quantum expected values of normally ordered functions are equal to the stochastic averages of the same functions after changing boson operators $(\hat{a}_m, \hat{a}_m^\dagger)$ by independent complex stochastic variables (α_m, α_m^+).

With this procedure, we have obtained a set of stochastic differential equations, (21) together with (74) and (76), ruling the evolution of the fields inside the cavity. However, the analysis of this model turns out to be quite involved.

A simpler model retaining the essential ingredients consists in neglecting the temporal evolution of the pumping fields, or further, considering the undepletion limit for the pump. As follows from (74a) and (74b) applied to (21), this will be a reasonable approximation whenever the gain g, (16), is small enough as for $|\alpha_\pm| \ll |\alpha_{1,2}|$. In such a case, one can safely neglect the amplitude variation of the pump modes. Of course, in doing that some of the dynamical richness of the system is lost, but the approximation simplifies very much the analysis of the rotational symmetry breaking that is fully retained by the simplified model.

Hence, in the following, we will study a reduced model in which the pump fields are taken to be equal (and real without loss of generalization), i.e., we take

$$\alpha_1 = \alpha_2 \equiv \rho \in \mathbb{R}. \tag{25}$$

D. Reduced Model

Under the assumption that the pump fields remain constant, thus satisfying (25), the Fokker–Planck equation of the system looks like (19), but with simpler diffusion matrix and drift vector.

From the general expressions given in Appendix B, it is easy to obtain that the diffusion matrix reads now

$$\mathcal{D} = \begin{pmatrix} \mathcal{D}^{(-)} & 0 \\ 0 & \mathcal{D}^{(+)} \end{pmatrix} \tag{26a}$$

$$\mathcal{D}^{(-)} = ig \begin{pmatrix} \alpha_+^2 & 2\alpha_+\alpha_- + 2\rho^2 \\ 2\alpha_+\alpha_- + 2\rho^2 & \alpha_-^2 \end{pmatrix} \tag{26b}$$

($\mathcal{D}^{(+)}$ is like $\mathcal{D}^{(-)}$ but swapping α_k and α_k^+, and changing i by $-i$), and that the components of the drift vector are

$$A_{\alpha_\pm} = -(\gamma_s + i\delta)\alpha_\pm + ig\left(\alpha_\pm^+ \alpha_\pm + 2\alpha_\mp^+ \alpha_\mp + 4\rho^2 \right) \alpha_\pm + 2i\rho^2 \alpha_\mp^+ \tag{27}$$

being $A_{\alpha_\pm^+}$ like $A_{\alpha_\pm}$ after swapping α_k and α_k^+, and changing i by $-i$.

Like before, from this Fokker–Planck equation, a set of Langevin equations can be obtained. Nevertheless, it will be useful to introduce the following change of variables and parameters (we note that the phase factor ψ appearing in the rescaled fields is introduced to make the stationary solutions of the classical equations satisfy $\bar{\beta}_- = \bar{\beta}_+^*$, see (35), which simplifies the quantum analysis)

$$\beta_\pm = \sqrt{\frac{g}{\gamma_s}} \alpha_\pm e^{-i\psi}, \qquad \beta_\pm^+ = \sqrt{\frac{g}{\gamma_s}} \alpha_\pm^+ e^{i\psi},$$
$$p = 2\frac{g}{\gamma_s}\rho^2, \qquad \Delta = \frac{\delta}{\gamma_s}, \qquad \kappa = \frac{g}{\gamma_s}, \qquad T = \gamma_s t \tag{28}$$

with

$$\sin 2\psi = \sqrt{\frac{\gamma_s}{g}} \frac{1}{2\rho} = \frac{1}{\sqrt{2p}} \tag{29}$$

in terms of which the Langevin equations for the reduced model read

$$\dot{\beta}_\pm = -(1 + i\Delta)\beta_\pm + i\left(\beta_\pm^+ \beta_\pm + 2\beta_\mp^+ \beta_\mp + 2p \right) \beta_\pm + ipe^{-2i\psi} \beta_\mp^+ + \tilde{\mathcal{B}}_{\beta_\pm, j} \xi_j(T) \tag{30}$$

plus the corresponding equations for $\beta_\pm^+$, which are like those for $\beta_\pm$ as described earlier after swapping β_k and β_k^+, and changing i by $-i$. The overdot indicates derivative with respect to the adimensional time T, and the four components of the noise vector $\boldsymbol{\xi}$ satisfy properties (22) now for the adimensional time T. As for the noise matrix $\tilde{\mathcal{B}}$, it can be obtained from $\tilde{\mathcal{D}} = \tilde{\mathcal{B}} \cdot \tilde{\mathcal{B}}^T$ as usual, but now using the diffusion matrix after introducing the changes (28), which reads as (26a) but with

$$\tilde{\mathcal{D}}^{(-)} = i\kappa \begin{pmatrix} \beta_+^2 & 2\beta_+\beta_- + p^2 e^{-2i\psi} \\ 2\beta_+\beta_- + p^2 e^{-2i\psi} & \beta_-^2 \end{pmatrix} \tag{31}$$

and with $\mathcal{D}^{(+)}$ like $\mathcal{D}^{(-)}$ but swapping β_k and β_k^+, and changing i by $-i$. In any case, there is no need to evaluate $\tilde{\mathcal{B}}$ at this moment.

Equation (30) constitutes the model that we analyze in detail shortly.

III. Classical Limit

Before addressing the analysis of quantum fluctuations, we need to know the classical steady states of the system as well as their stability properties, and for doing that we must first write down the classical limit of (30). This is easily done by neglecting the noise terms and by making $\beta_j^+ = \beta_j^*$ in the quantum Langevin equation (30). We obtain the following set of two complex ordinary differential equations for the signal classical fields amplitudes $\beta_\pm$:

$$\dot{\beta}_\pm = -\left[1 + i\left(\Delta - |\beta_\pm|^2 - 2|\beta_\mp|^2 - 2p\right)\right]\beta_\pm + ipe^{-2i\psi}\beta_\mp^*. \tag{32}$$

Due to rescaling (28), we can appreciate that the classical dynamics of the system is governed by just two parameters, namely the normalized detuning Δ and pump strength p. We pass now to study the stationary solutions of (32) as well as their stability properties.

Equation (32) has two steady states. First, there is the trivial steady state $\beta_\pm = 0$. It is easy to show that its stability is governed by the eigenvalues

$$\lambda_\pm = -1 \pm \sqrt{p^2 - (\Delta - 2p)^2} \tag{33}$$

what implies that the trivial solution is stable except when the pump amplitude p verifies $p_- < p < p_+$ with

$$p_\pm = \frac{1}{3}(2\Delta \pm \sqrt{\Delta^2 - 3}) \tag{34}$$

in which case the trivial solution becomes linearly unstable because $\mathrm{Re}(\lambda_+) > 0$. Note that a prerequisite for the destabilization of the trivial solution is that $\Delta > \sqrt{3}$ (p is positive).

At the instability points $\mathrm{Re}(\lambda_+) = 0$, the system passes from the trivial state to the nontrivial one, which reads

$$\bar{\beta}_\pm = \mu e^{\mp i\theta} \tag{35}$$

with

$$\mu^2 = \frac{1}{3}(\Delta - 2p \pm \sqrt{p^2 - 1}) \tag{36}$$

and where θ is half the phase difference between the two Laguerre–Gauss modes amplitudes, and is not fixed by (32), hence being arbitrary. In Fig. 2(a), this solution is shown as a function of p for three values of Δ.

Note first that there are two possible values for μ. It is easy to demonstrate that the solution with the minus sign in front of the square root [dashed lines in Fig. 2(a)] is always unstable, while the solution with the plus sign [continuous lines in Fig. 2(a)] is stable within all its domain of existence. Note also that while the sum of the phases of the two Laguerre–Gauss modes amplitudes

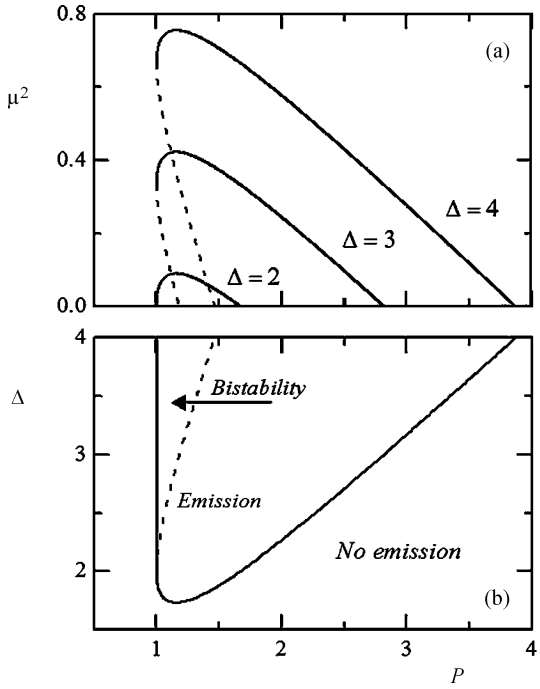

Fig. 2. (a) Intensity of the emitted classical signal beam as a function of the pump strength p for the indicated values of the detuning Δ. Continuous (dashed lines) lines indicate linearly stable (unstable) solutions. (b) Domain of existence and stability of the solutions. The nontrivial solution exists in the domain limited by the two continuous lines. The trivial solution is stable to the left of the dashed line and to the right of the right continuous line. Hence, the system is bistable in the region between the dashed line and the left continuous line, marked in the figure.

is fixed to zero [this is due to the change of variables (28)], their phase difference θ is an arbitrary quantity, which reflects the rotational invariance of the system as this phase difference determines the orientation in the transverse plane of the emitted Hermite–Gauss mode, see (38) later.

From (36), it follows that the necessary condition for the existence of the nontrivial solution is $p > 1$, and its domain of existence is determined by the condition

$$\Delta > 2p - \sqrt{p^2 - 1}. \tag{37}$$

Note that this inequality can be satisfied only if $\Delta > \sqrt{3}$, in agreement with our analysis of the trivial solution. In Fig. 2(b), we represent this domain of existence as well as the domain of stability of the trivial solution (see Fig. 2(b) caption).

From all the aforementioned equations, we see that the classical nontrivial state's slowly varying amplitude can be written as

$$\begin{aligned} A_s^{\mathrm{class}}(\mathbf{r}) &= \mu\left[e^{-i\theta}L_+(\mathbf{r}) + e^{+i\theta}L_-(\mathbf{r})\right] \\ &= \left[\frac{2}{3}(\Delta - 2p + \sqrt{p^2 - 1})\right]^{1/2} H_{10}^{\theta}(\mathbf{r}). \end{aligned} \tag{38}$$

This solution corresponds to a Hermite–Gauss mode rotated an angle θ with respect to the x-axis, being the value of this angle arbitrary. As already noted, the arbitrariness of θ is the consequence of the rotational symmetry of the system: as the pumping modes are rotationally symmetric, as the cavity is, the signal

TEM_{10} Hermite–Gauss mode cannot have any preferred orientation, and thus, all orientations are equally likely. This property is essential for the results we present shortly for quantum fluctuations.

Finally, note that the fact that the emission takes place in a TEM_{10} mode, allows us to distinguish between two different modes: the $H^{\theta}_{10}(\mathbf{r})$ mode, which is the classically generated one, and its orthogonal mode $H^{\theta}_{01}(\mathbf{r})$, which is empty of photons at the classical level. In the following, we shall refer to these modes as the *bright* and *dark* modes, and will define collective indexes $\mathrm{b} = (10, \theta)$ and $\mathrm{d} = (01, \theta)$.

IV. Quantum Analysis

We return to the quantum description of the system. In the following sections, we first derive the linearized Langevin equations and then solve them with the method introduced in [14] and [15] and further used in [7]–[9]. Next, we show the most outstanding quantum properties of the system: after proving that the bright mode is rotating randomly in the transverse plane, we show that the dark mode has perfect noise reduction in one of its quadratures.

A. Linearization of the Langevin Equations

We linearize (30), a valid approximation in the large photon number limit, and thus, appropriate for our purposes as we are going to analyze quantum fluctuations around the above threshold solution (35). Consequently, we write

$$\beta_{\pm} = \left[\mu + b_{\pm}(T)\right] e^{\mp i\theta(T)} \tag{39a}$$

$$\beta^{+}_{\pm} = \left[\mu + b^{+}_{\pm}(T)\right] e^{\pm i\theta(T)} \tag{39b}$$

where the phase difference θ appears explicitly in order to keep the b's small. Then, by assuming that b_j, ξ_j, and $\dot{\theta}$ are small quantities, we easily arrive to the following linearized Langevin equations:

$$\dot{\mathbf{b}} + iN_0\mu\dot{\theta}\mathbf{v}_0 = \mathcal{L}\mathbf{b} + \mathcal{K}\bar{\mathcal{B}}\boldsymbol{\xi} \tag{40}$$

where

$$\mathbf{b} = \mathrm{col}\left(b_+, b_-, b^{+}_{+}, b^{+}_{-}\right) \tag{41a}$$

$$\mathbf{v}_0 = \frac{1}{N_0}\mathrm{col}\left(-1, 1, 1, -1\right) \tag{41b}$$

where N_0 is a normalization factor (see (51) shortly) and $\mathcal{L}$ is a matrix with elements

$$\mathcal{L}_{ij} = \left.\frac{\partial A_i}{\partial \beta_j}\right|_{\boldsymbol{\beta}=\bar{\boldsymbol{\beta}}} \tag{42}$$

and $\mathcal{K}$ is the diagonal matrix

$$\mathcal{K} = \mathrm{diag}(e^{i\theta}, e^{-i\theta}, e^{-i\theta}, e^{i\theta}). \tag{43}$$

Finally, $\bar{\mathcal{B}}$ refers to matrix $\tilde{\mathcal{B}}$ evaluated at the stationary state (35). Its expression can be derived from $\bar{\mathcal{D}} = \bar{\mathcal{B}} \cdot \bar{\mathcal{B}}^T$ with

$$\bar{\mathcal{D}} = \tilde{\mathcal{D}}|_{\boldsymbol{\beta}=\bar{\boldsymbol{\beta}}} = \begin{pmatrix} \bar{\mathcal{D}}^{(-)} & 0 \\ 0 & \bar{\mathcal{D}}^{(+)} \end{pmatrix} \tag{44a}$$

$$\bar{\mathcal{D}}^{(-)} = \left[\bar{\mathcal{D}}^{(+)}\right]^* = i\kappa \begin{pmatrix} \mu^2 e^{-2i\theta} & 2\mu^2 + pe^{-2i\psi} \\ 2\mu^2 + pe^{-2i\psi} & \mu^2 e^{2i\theta} \end{pmatrix}. \tag{44b}$$

After some algebra, it is easy to show that $\bar{\mathcal{B}}$ can be written as

$$\bar{\mathcal{B}} = \begin{pmatrix} \bar{\mathcal{B}}^{(-)} & 0 \\ 0 & \bar{\mathcal{B}}^{(+)} \end{pmatrix} \tag{45a}$$

$$\bar{\mathcal{B}}^{(-)} = \left[\bar{\mathcal{B}}^{(+)}\right]^* = \begin{pmatrix} ae^{-i\theta} & be^{-i\theta} \\ ce^{i\theta} & de^{i\theta} \end{pmatrix} \tag{45b}$$

where elements (a, b, c, d) are independent of θ, and satisfy the following relations:

$$a^2 + b^2 = c^2 + d^2 = i\kappa\mu^2 \tag{46a}$$

$$ac + bd = i\kappa(2\mu^2 + pe^{-2i\psi}). \tag{46b}$$

B. Solving the Linearized Langevin Equations

In order to solve the linearized Langevin equation (40), we follow a procedure analogous to that in [7]–[9], [14] and [15]. The method consists in projecting (40) into the eigensystem of the linear operator $\mathcal{L}$. This provides a direct way for the evaluation of the quantum fluctuations of the relevant physical quantities, as we show shortly.

Operator $\mathcal{L}$ has not an orthonormal but a biorthonormal eigensystem, i.e., there is an eigensystem of operators $\mathcal{L}$ and $\mathcal{L}^{\dagger}$ verifying

$$\mathcal{L}\mathbf{v}_j = \lambda_j\mathbf{v}_j \qquad \mathcal{L}^{\dagger}\mathbf{w}_j = \lambda^*_j\mathbf{w}_j \tag{47a}$$

such that

$$\mathbf{w}^*_m \cdot \mathbf{v}_n = \delta_{mn}. \tag{48}$$

The quantitative result of the analysis of $\mathcal{L}$ and $\mathcal{L}^{\dagger}$ is that their four eigenvalues read

$$\lambda_0 = 0, \quad \lambda_1 = -2, \tag{49a}$$

$$\lambda_2 = \lambda_2(p, \Delta), \quad \lambda_3 = -2 - \lambda_2. \tag{49b}$$

We see that eigenvalue λ_0 is always null. This means that its corresponding eigenvector, which is said to be a Goldstone mode (its expression is given shortly), is neutrally stable, i.e., its associated variable can take any possible value. Of course this reflects the indeterminacy of the phase difference between the two Laguerre–Gauss modes, θ, or what is the same, the indeterminacy of the orientation of the Hermite–Gauss output mode in the transverse plane. Hence, the null eigenvalue implies that the fluctuations introduced by quantum noise in this orientation are not damped and, hence, that quantum noise will induce arbitrary rotations of the Hermite–Gauss output mode in the transverse plane. Thus, the breaking of the rotational symmetry of the system introduced by the appearance of the Hermite–Gauss mode is, in a sense, counteracted by quantum noise by making

possible any possible orientation. Together with $\lambda_0 = 0$, there is the companion eigenvalue $\lambda_1 = -2$. Its corresponding eigenvector (see shortly) is consequently maximally damped irrespective of the system's parameter values. As we show shortly, it is the observable associated to the eigenvector corresponding to λ_1 the one that is perfectly squeezed.

On the other hand, the two other eigenvalues, λ_2 and λ_3, are complex in general; nevertheless, they reach the values 0 and -2 at the bifurcation points (i.e., at the points in the parameter space separating the regions where the steady state solution (35) exist or not). Consequently, their associated eigenvectors are those exhibiting the usual squeezing occurring only at the bifurcations. This squeezing is not perfect (it seems perfect only owed to the linearized treatment) and degrades quickly as the system parameters are brought apart from the bifurcation points. We shall not analyze this squeezing here because there is not any relevant new feature in it with respect to what has been described many times in other nonlinear optical cavities. Hence, in the following, we concentrate on the analysis of the modes associated to the first two eigenvalues that are the ones connected with the rotational symmetry breaking.

It is not difficult to show that the eigenvectors of $\mathcal{L}$ associated to λ_0 and λ_1 are

$$\mathbf{v}_0 = \frac{1}{N_0}\mathrm{col}(-1,1,1,-1) \tag{50a}$$

$$\mathbf{v}_1 = \frac{1}{N_0}\mathrm{col}(e^{i\phi_0}, -e^{i\phi_0}, e^{-i\phi_0}, -e^{-i\phi_0}) \tag{50b}$$

with

$$N_0 = -4\cos\phi_0 \tag{51}$$

a normalization factor and ϕ_0 a real quantity given by

$$e^{2i\phi_0} = \frac{\mu^2 + pe^{-i\psi}}{2(\mu^2+p) - (\Delta + i)}. \tag{52}$$

As for the eigenvectors of $\mathcal{L}^\dagger$, they read

$$\mathbf{w}_0 = \mathrm{col}(e^{i\phi_0}, -e^{i\phi_0}, -e^{-i\phi_0}, e^{-i\phi_0}) \tag{53a}$$

$$\mathbf{w}_1 = \mathrm{col}(1,-1,1,-1). \tag{53b}$$

Once these eigenvectors of the linear operator are known, we proceed to project quantum fluctuations onto them. We define projections

$$c_j = \mathbf{w}_i^* \cdot \mathbf{b}, \qquad j = 0, 1. \tag{54}$$

Note that these projections can be easily related with the fluctuations of the quadratures associated to the bright and dark modes H_{10}^θ and H_{01}^θ, see (8). In particular, by using (8) and (39), it is easy to arrive at

$$X_{\mathrm{d}}^{\phi_0} = \frac{i}{\sqrt{2}}c_0, \qquad X_{\mathrm{d}}^{\pi/2} = \frac{1}{\sqrt{2}}c_1. \tag{55}$$

Next, we project the linearized Langevin equation (40). By multiplying them by $\mathbf{w}_j^*$ on the left, we get

$$\dot{\theta}(T) = \frac{1}{iN_0\mu}\mathbf{w}_0^*\mathcal{K}\bar{\mathcal{B}}\boldsymbol{\xi}(T) \tag{56a}$$

$$\dot{c}_1(T) = \lambda_1 c_1(T) + \mathbf{w}_1^*\mathcal{K}\bar{\mathcal{B}}\boldsymbol{\xi}(T) \tag{56b}$$

where we have taken $c_0 = 0$ (this can be done because the arbitrary phase θ can be conveniently redefined in order to collect the information on this mode). We note that although $\mathcal{K}$ and $\bar{\mathcal{B}}$ depend on phase θ, $\mathcal{K}\bar{\mathcal{B}}$ does not, as can be checked from (43) and (45). Hence, these equations are truly decoupled for θ and c_1.

In the stationary limit, i.e., for large T, the solution of the earlier equations reads

$$\theta(T) = \theta(0) + \frac{\mathbf{w}_0^*\mathcal{K}\bar{\mathcal{B}}}{iN_0\mu}\int_0^T dT'\boldsymbol{\xi}(T') \tag{57a}$$

$$c_1(T) = \mathbf{w}_1^*\mathcal{K}\bar{\mathcal{B}}\int_0^T dT'\boldsymbol{\xi}(T')e^{-2(T'-T)}. \tag{57b}$$

Finally, we evaluate, for later purposes, the correlation spectrum of c_1. From the formal solution (57b), it is straightforward to prove that the correlation function of this projection reads

$$C_1(\tau) = \langle c_1(T)c_1(T+\tau)\rangle = \frac{\mathbf{w}_1^*\mathcal{K}\bar{\mathcal{D}}\mathcal{K}\mathbf{w}_1^*}{4}e^{-2|\tau|}. \tag{58}$$

It is not difficult to obtain that $\mathbf{w}_1^*\mathcal{K}\bar{\mathcal{D}}\mathcal{K}\mathbf{w}_1^* = -4\kappa$, and then the spectrum of correlation $C_1(\tau)$ turns out to be

$$\tilde{C}_1(\omega) = \int_{-\infty}^{+\infty} d\tau e^{-i\omega\tau}C_1(\tau) = -\frac{\kappa}{4+\omega^2}. \tag{59}$$

C. Dynamics of the Bright Mode's Orientation

We first analyze the dynamics of the output pattern orientation, governed by θ. Equation (57a) shows that the phase θ diffuses with time what means that the orientation of the classical mode in which emission occurs, (38), exhibits a random walk. Then, although the mode orientation is well defined at every instant, it can be understood that the pattern orientation is undefined as after some time any value between 0 and 2π could be found. This is what we understand when we say that the orientation of the output pattern is undetermined.

It is important to see how much does θ diffuse. From (57a), it is straightforward to show that the variance of θ is given by

$$\langle \delta\theta(T)^2\rangle = d_\theta T \tag{60a}$$

where we have used the notation $\delta A = A - \langle A\rangle$, and

$$\begin{aligned} d_\theta &= -\frac{\mathbf{w}_0^*\mathcal{K}\bar{\mathcal{D}}\mathcal{K}\mathbf{w}_0^*}{N_0^2\mu^2} \\ &= \kappa\frac{\mu^2\sin 2\phi_0 + p\sin[2(\phi_0+\psi)]}{4\mu^2\cos^2\phi_0} \end{aligned} \tag{61}$$

with ψ, μ, and ϕ_0 being given by (29), (36), and (52).

In Fig. 3, we represent $D \equiv d_\theta/\kappa$ as a function of the pump strength p for several values of Δ. Note that for $\mu \to 0$ (i.e., at the supercritical bifurcation that occurs in the upper branch of the domain of existence of (35), see Fig. 2), $D \to \infty$. This is an intuitive result because when the output mode mean photon number is close to zero, the pattern orientation can be abruptly changed with the addition of a single couple of photons. As the system is brought apart from this bifurcation, the mean number

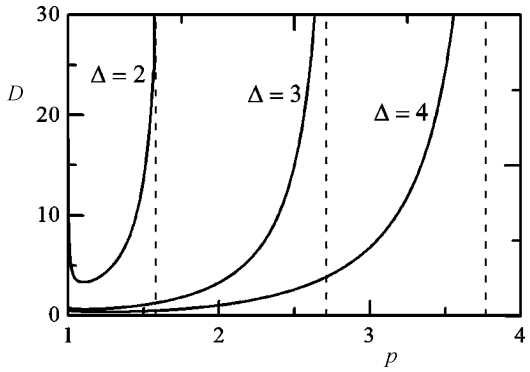

Fig. 3. Dependence of the normalized diffusion constant $D = d_\theta/\kappa$ as a function of the pump strength p for the values of the detuning indicated in the figure. The vertical dashed lines indicate the values of p where the nontrivial solution ceases to exist.

of photons rapidly increases and, consequently, it is more difficult for the fluctuation to change the orientation of the pattern, what is obviously consistent with the rapid decrease of D. As for the quantitative value note that, except very close to the supercritical bifurcations, D is a quantity of order one what means that the diffusion constant d_θ is basically of the same order of magnitude as $\kappa = g/\gamma_s$, which we have assumed to be a very small number. Consequently, although the TEM output mode is randomly rotating in the transverse plane, the rotation is very slow except very close to the supercritical bifurcation points.

D. Noncritical Squeezing Properties of the Dark Mode

Now we focus on the main result of the present paper. We show shortly that the dark mode has complete noise reduction on its phase quadrature irrespective of the system parameters. To this aim we evaluate its quadrature fluctuations as measured in an homodyne detection experiment. As it is well known (see, e.g., [16]), quadrature fluctuations outside the cavity are given by the noise spectrum, which for a general problem quadrature $\hat{X}_m^\varphi$ (m refers to any of the transverse modes of our system) is given by

$$V^{\text{out}}(\omega; X_m^\varphi) = 1 + S_m^\varphi(\omega) \tag{62}$$

with $S_m^\varphi(\omega)$ the squeezing spectrum that, after taking into account our rescaling (28), can be written as

$$S_m^\varphi(\omega) = \frac{2}{\kappa}\int_{-\infty}^{+\infty} d\tau e^{-i\omega\tau}\left\langle \delta X_m^\varphi(T)\delta X_m^\varphi(T+\tau)\right\rangle. \tag{63}$$

Defined in this way, $V^{\text{out}}(\bar{\omega}) = 0$ means complete absence of fluctuations at $\omega = \bar{\omega}$, while $V^{\text{out}}(\bar{\omega}) = 1$ means that fluctuations at $\omega = \bar{\omega}$ are those corresponding to the vacuum state.

In the homodyning, the spatial profile of the local oscillator field (LOF) selects the transverse mode to be measured, while its phase selects a particular mode's quadrature. In what follows we suppose that the LOF is perfectly matched to the dark mode's profile $H_{01}^\theta(\mathbf{r})$. As we saw in (55), the independent quadratures of this mode are $X_{\text{d}}^{\phi_0}$ and $X_{\text{d}}^{\pi/2}$, from which we can build a general quadrature as

$$X_{\text{d}}^\varphi = \frac{1}{\cos\phi_0}\left[X_{\text{d}}^{\phi_0}\cos\varphi + Y_{\text{d}}\sin(\varphi-\phi_0)\right]. \tag{64}$$

This expression is readily obtained from the more common expressions $X_{\text{d}}^\varphi = X_{\text{d}}^0\cos\varphi + X_{\text{d}}^{\pi/2}\sin\varphi$ and $X_{\text{d}}^{\phi_0} = X_{\text{d}}^0\cos\phi_0 + X_{\text{d}}^{\pi/2}\sin\phi_0$.

Hence, by using the relation between the independent quadratures and the projections c_j (55), and remembering (59) and that $c_0 = 0$, it is trivial to find the noise spectrum of this general quadrature, which reads

$$V^{\text{out}}(\omega; X_{\text{d}}^\varphi) = \frac{\cos^2\varphi + \sin^2(\varphi-\phi_0)}{\cos^2\phi_0} - \frac{\sin^2(\varphi-\phi_0)}{\cos^2\phi_0}\frac{1}{1+(\omega/2)^2}. \tag{65}$$

This expression shows that the quantum properties of the dark mode of the current system are exactly the same as that found in [7] and [8] for the case of a DOPO cavity: at $\omega = 0$, $V^{\text{out}}(\omega = 0; X_{\text{d}}^\varphi) = \cos^2\varphi/\cos^2\phi_0$, and thus, it has complete absence of fluctuations on its phase quadrature ($\varphi = \pi/2$), while another of its quadratures ($\varphi = \phi_0$ in our case) carries only with vacuum fluctuations. Any other quadrature having φ between $\pi/2$ and ϕ_0 is squeezed below the vacuum level, though the squeezing level is smaller as φ approaches to ϕ_0. These results are independent of the system parameters, what we expected as the noise reduction relies on the rotational symmetry breaking only.

It could seem that this result violates the uncertainty principle, as the product of the noise spectra corresponding to two orthogonal quadratures is below unity. However, in [8], we have proven that this is actually not the case, as the canonical pair of the squeezed quadratures is not another quadrature, but the orientation of the dark mode θ, which is indeed undetermined in the long time term.

V. Conclusion

We have proposed a model for a Kerr cavity in which a spontaneous rotational symmetry breaking occurs when the system is beyond the emission threshold: the nonlinear cavity has a perfect rotational symmetry and is pumped by Gaussian beams, but the emitted signal field has the shape of a TEM_{10} mode that breaks the rotational symmetry. We have demonstrated in a special simple limit (in which the pumping fields are taken as constants) that the rotational symmetry breaking implies: 1) the diffusion of the output mode orientation and 2) the perfect squeezing of the phase quadrature of the TEM_{10} mode that is rotated $\pi/2$ with respect to the signal TEM_{10} mode. These results are in perfect agreement with our previous proposal of the symmetry breaking mediated squeezing in a DOPO model [7], [8]. The interest of the results here presented are twofold. On one hand, we are proposing a system different to that of [7]and [8] for the possible observation of the phenomenon, thus showing that the results in [7] and [8] are quite general. On the other hand, rotational symmetry could be broken in a DOPO cavity if angular phase matching is necessary, as in this case, the nonlinear crystal axis is rotated a certain angle with respect to the cavity

axis, a problem that does not exist in the case of a $\chi^{(3)}$ nonlinear medium as phase matching is easier to obtain.

As for the particular model we have proposed, in its formulation we have assumed a confocal cavity, as in this cavity type the required resonances are verified. Note, however, that the ingredients that are essential for the phenomenon of rotational symmetry breaking mediated squeezing generation are: 1) rotational invariance and 2) that the signal field photons have nonnull OAM. Then, the dynamics of the pumping modes is irrelevant except for the quantitative details. In this sense, the use of a confocal cavity is not essential and any other $\chi^{(3)}$ cavity in which the signal modes are the right ones could exhibit the described phenomenon. Then, this phenomenon could possibly be observed in other $\chi^{(3)}$ cavities such as, e.g., fiber resonators. We wish to note that related optical fiber (or other Kerr media) devices leading to optical parametric oscillation have been demonstrated and very likely present interesting quantum properties [17]–[19].

Another comment we would like to add concerns the undepleted pump approximation. How would the dynamics of the pumping modes affect the results we have derived? The inclusion of the pumping fields equations in the study would obviously introduce more eigenvalues (the ones corresponding to the stability of these modes) and would modify some of the eigenvalues governing the dynamics of the signal modes, but would not modify the existence of a Goldstone mode once the signal field is switched on (as it appears due to the symmetry breaking). Hence, as far as the dynamics of the pumping modes does not destroy completely the stability of the continuous wave (CW) signal field emission, wherever the signal modes are stable the phenomenon will be present. It could well happen that the general model exhibits Hopf bifurcations that would reduce the domain of stable existence of the CW signal modes, but there will be a finite domain of stability for these modes and within it there will be the perfect squeezing properties we have described in our work.

We would finally stress two important features. In [7], we demonstrated for a DOPO model that small imperfections in the rotational symmetry do not lead but to a small degradation of the squeezing level (e.g., a ratio 2:1 between the cavity losses affecting two orthogonal directions in the transverse plane still allows for 10 dB of noise reduction). On the other hand, in [8], we have numerically demonstrated for the same DOPO model that the rotational symmetry breaking mediated squeezing is perfect beyond the linear approximation. These conclusions should also hold for the system presented here.

APPENDIX A

For the sake of clarity, we find it convenient to review the main properties of the cavity modes in a Fabry–Perot resonator with spherical mirrors (see, e.g., [10] for more details). Within the paraxial approximation, it is well known that the Laguerre–Gauss modes form a complete set of spatial modes describing the light inside the resonator. Let R_1 and R_2 denote the curvature radius of the cavity mirrors, and $L = L_{\rm geo} - (1 - 1/n)l_{\rm m}$ the effective cavity length, being $L_{\rm geo}$ the geometrical length of the resonator, and $l_{\rm m}$ and n the length and refractive index, respectively, of the $\chi^{(3)}$ medium. Then, the Laguerre–Gauss modes at the resonator waist plane can be written as

$$\Psi_p^{\pm l}(\mathbf{r}) = \mathcal{N}_p^l u_p^l(r)\exp(\pm il\phi) \tag{66}$$

with $\mathbf{r} = (x, y)$ the transverse coordinates being $\mathbf{r} = r(\cos\phi, \sin\phi)$ its polar decomposition, $\mathcal{N}_p^l$ a normalization factor and

$$u_p^l(r) = \frac{1}{w}\left(\frac{\sqrt{2}r}{w}\right)^l L_p^l\left(\frac{2r^2}{w^2}\right)e^{-r^2/w^2} \tag{67}$$

L_p^l being the modified Laguerre polynomial with radial and polar indexes $p, l \in \mathbb{N}$, which are given by Rodrigues formula

$$L_p^l(v) = \frac{1}{p!}e^v\frac{1}{v^l}\frac{d^p}{dv^p}(e^{-v}v^l v^p). \tag{68}$$

By choosing the normalization factor as

$$\mathcal{N}_p^l = \sqrt{\frac{2}{\pi}\frac{p!}{(p+l)!}} \tag{69}$$

the following orthogonality relation holds:

$$\int_0^{2\pi} d\phi \int_0^{\infty} r dr \left[\Psi_p^{\pm l}(\mathbf{r})\right]^* \Psi_{p'}^{\pm l'}(\mathbf{r}) = \delta_{ll'}\delta_{pp'}. \tag{70}$$

The beam spot size at the cavity waist w is given by

$$w^2 = \frac{2cL}{\omega}\frac{\sqrt{g_1 g_2(1 - g_1 g_2)}}{g_1 + g_2 - 2g_1 g_2} \tag{71}$$

with $g_j = 1 - L/R_j$ and ω the beam frequency.

The Laguerre–Gauss basis is recommended in order to visualize the OAM of the field, as these modes are eigenstates of the OAM operator $-i\partial_\phi$ with eigenvalues $\pm l$. Concerning the resonance frequency of the different $\Psi_p^{\pm l}$ modes, they are different in general for each mode. Concretely

$$\omega_{qpl} = \frac{\pi c}{L}\left(q + \frac{1 + 2p + l}{\pi}\arccos \pm\sqrt{g_1 g_2}\right) \tag{72}$$

with q an integer (different $q's$ correspond to different longitudinal cavity modes), and the plus sign must be used for $g_1 > 0$ (and hence $g_2 > 0$ if the resonator must be stable), while the minus sign appears in the opposite case ($g_1 < 0$ and $g_2 < 0$).

Hence, cavity modes having the same *family order* $f = 2p + l$ have the same frequency and are said to be members of the same family f (in the following we will denote this frequency by ω_{qf}). It is clear that family f consists of the set of $f + 1$ Laguerre–Gauss modes $\{\Psi_{(f-l)/2}^{\pm l}\}$ with $l = f, f - 2, \ldots, l_0$, having OAM $\pm f, \pm(f - 2), \ldots, \pm l_0$. The lower OAM modes have $l_0 = 0$ or 1 for even or odd f, respectively.

As we stated in the model section, we need the resonator tuned in such a way that the resonance frequency of a $f = 1$ family lies in the middle between that two fundamental $l = 0$ modes. To this aim, resonators satisfying $g_1 \cdot g_2 = 0$ are the perfect ones, as they satisfy this condition and in addition give

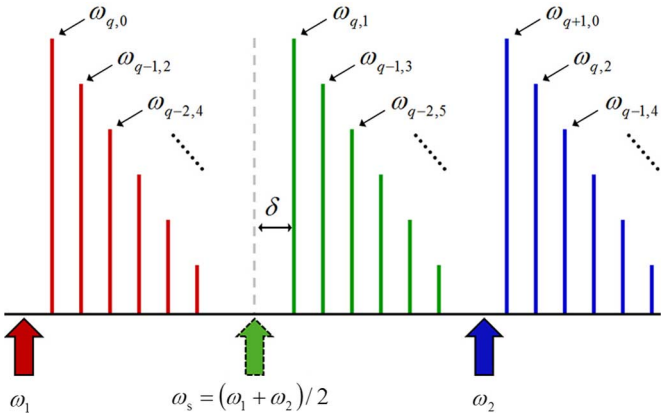

Fig. 4. Modal spectrum of a nearly symmetric, nearly confocal cavity. In the figure, the values $g_1 = g_2 = -0.1$ have been chosen. Pump frequencies are denoted by ω_1 and ω_2, while the generated signal frequency is ω_s, having detuning δ with respect to the $f = 1$ family resonance frequency.

the largest splitting between the $f = 0$ and $f = 1$ modes (half the free spectral range, i.e., $\pi c/2L$). However, the situation is not ideal, as these resonators also satisfy

$$\omega_{q,f} = \omega_{q-1,f+2} \tag{73}$$

and hence modes laying in higher odd families have the same resonance frequency as that of the $f = 1$ one. Nevertheless, for the reasons we gave in the beginning of the model section, the existence of these mode should not disguise in any way the phenomenon we study in this work.

On the other hand, in the classical analysis section, we show that in order to generate the desired TEM_{10} mode, it is needed some detuning of the pump field's frequencies with respect to the cavity resonances (a positive detuning indeed, i.e., the cavity resonance must be larger than the pump frequencies). This feature allows us to relax the restrictions onto the cavities that are useful for our purposes. To see how this is the case, we show in Fig. 4 the resonance structure of a cavity with $g_1 \cdot g_2 \simeq 0$. The modes laying in families of the same parity have no longer the same resonance frequency, and they get split. To prevent any $f \neq 1$ family taking part in the nonlinear competition, we must require in addition g_1 and g_2 to be negative, as in this case the $f = 1$ family has the lowest detuning (δ in Fig. 4) with respect to the signal frequency (ω_s in Fig. 4).

Hence, we see that although our model has been considered with a confocal cavity having $g_1 = g_2 = 0$, the whole family of nearly symmetric, nearly confocal cavities could be also used.

APPENDIX B

The components of the drift vector in (19) read

$$\begin{aligned} A_{\alpha_1} =& \mathcal{E}_p - (\gamma_1 + i\delta)\alpha_1 + 4ig\alpha_2^+\alpha_2\alpha_1 \\ &+ 2ig\left(\alpha_1^+\alpha_1^2 + \alpha_+^+\alpha_+\alpha_1 + \alpha_-^+\alpha_-\alpha_1 \right. \\ &\left. + \alpha_2^+\alpha_+\alpha_-\right) \end{aligned} \tag{74a}$$

$$\begin{aligned} A_{\alpha_2} =& \mathcal{E}_p - (\gamma_2 + i\delta)\alpha_2 + 4ig\alpha_1^+\alpha_1\alpha_2 \\ &+ 2ig\left(\alpha_2^+\alpha_2^2 + \alpha_+^+\alpha_+\alpha_2 + \alpha_-^+\alpha_-\alpha_2 \right. \\ &\left. + \alpha_1^+\alpha_+\alpha_-\right) \end{aligned} \tag{74b}$$

$$\begin{aligned} A_{\alpha_+} =& -(\gamma_s + i\delta)\alpha_+ + ig\alpha_+^+\alpha_+^2 \\ &+ 2ig\left(\alpha_-^+\alpha_-\alpha_+ + \alpha_1^+\alpha_1\alpha_+ + \alpha_2^+\alpha_2\alpha_+ \right. \\ &\left. + \alpha_-^+\alpha_1\alpha_2\right) \end{aligned} \tag{74c}$$

$$\begin{aligned} A_{\alpha_-} =& -(\gamma_s + i\delta)\alpha_- + ig\alpha_-^+\alpha_-^2 \\ &+ 2ig\left(\alpha_+^+\alpha_+\alpha_- + \alpha_1^+\alpha_1\alpha_- + \alpha_2^+\alpha_2\alpha_- \right. \\ &\left. + \alpha_+^+\alpha_1\alpha_2\right) \end{aligned} \tag{74d}$$

and the rest of components $A_{\alpha_k^+}$ are as A_{α_k} after complex-conjugating and swapping α_k and α_k^+. As for the diffusion matrix in (19), it reads

$$\mathcal{D} = 2ig\begin{pmatrix} \mathcal{D}^{(-)} & 0 \\ 0 & -\mathcal{D}^{(+)} \end{pmatrix} \tag{75}$$

being $\mathcal{D}^{(-)}$ a 4×4 matrix with elements

$$\mathcal{D}_{11}^{(-)} = \alpha_1^2, \quad \mathcal{D}_{22}^{(-)} = \alpha_2^2, \quad \mathcal{D}_{33}^{(-)} = \frac{\alpha_+^2}{2}, \quad \mathcal{D}_{44}^{(-)} = \frac{\alpha_-^2}{2} \tag{76a}$$

$$\mathcal{D}_{12}^{(-)} = \mathcal{D}_{21}^{(-)} = 2\alpha_1\alpha_2 + \alpha_+\alpha_- \tag{76b}$$

$$\mathcal{D}_{13}^{(-)} = \mathcal{D}_{31}^{(-)} = \alpha_1\alpha_+, \qquad \mathcal{D}_{14}^{(-)} = \mathcal{D}_{41}^{(-)} = \alpha_1\alpha_- \tag{76c}$$

$$\mathcal{D}_{23}^{(-)} = \mathcal{D}_{32}^{(-)} = \alpha_2\alpha_+, \qquad \mathcal{D}_{24}^{(-)} = \mathcal{D}_{42}^{(-)} = \alpha_2\alpha_- \tag{76d}$$

$$\mathcal{D}_{34}^{(-)} = \mathcal{D}_{43}^{(-)} = \alpha_1\alpha_2 + \alpha_+\alpha_- \tag{76e}$$

and $\mathcal{D}^{(+)}$ as $\mathcal{D}^{(-)}$ after swapping α_k and α_k^+.

ACKNOWLEDGMENT

The authors want to thank A. Aparici for his help with the final LaTeX code.

REFERENCES

[1] R. Loudon and P. L. Knight, "Squeezed light," *J. Mod. Opt.*, vol. 34, pp. 709–1020, 1987.
[2] D. F. Walls and G. J. Milburn, *Quantum Optics*. Berlin, Germany: Springer-Verlag, 1994.
[3] *Quantum Squeezing*, P. D. Drummond and Z. Ficek, Eds. Berlin, Germany: Springer-Verlag, 2004.
[4] S. L. Braunstein and P. van Loock, "Quantum information with continuous variables," *Rev. Mod. Phys.*, vol. 77, pp. 513–577, 2005.
[5] H. Vahlbruch, M. Mehmet, S. Chelkowski, B. Hage, A. Franzen, N. Lastzka, S. Goßler, K. Danzmann, and R. Schnabel, "Observation of squeezed light with 10-dB quantum-noise reduction," *Phys. Rev. Lett.*, vol. 100, pp. 033602-1–033602-4, 2008.
[6] Y. Takeno, M. Yukawa, H. Yonezawa, and A. Furusawa, "Observation of -9 dB quadrature squeezing with improvement of phase stability in homodyne measurement," *Opt. Expr.*, vol. 15, pp. 4321–4327, 2007.
[7] C. Navarrete-Benlloch, E. Roldán, and G. J. de Valcárcel, "Noncritically squeezed light via spontaneous rotational symmetry breaking," *Phys. Rev. Lett.*, vol. 100, pp. 203601-1–203601-4, 2008.
[8] C. Navarrete-Benlloch, A. Romanelli, E. Roldán, and G. J. de Valcárcel, "Non-critical squeezing in 2-transverse-mode optical parametric oscillators," arXiv: 0904.0049, 2009.
[9] C. Navarrete-Benlloch, G. J. de Valcárcel, and E. Roldán, "Generating highly squeezed hybrid Laguerre–Gauss modes in large fresnel number degenerate optical parametric oscillators," *Phys. Rev. A*, vol. 79, pp. 043820-1–043820-9, 2009, accepted for publication.
[10] N. Hodgson and H. Weber, *Laser Resonators and Beam Propagation*. New York: Springer-Verlag, 2005.
[11] P. D. Drummond and C. W. Gardiner, "Generalised P-representations in quantum optics," *J. Phys. A: Math. Gen.*, vol. 13, pp. 2353–2368, 1980.
[12] H. J. Carmichael, *Statistical Methods in Quantum Optics 1*. Berlin, Germany: Springer-Verlag, 1999.
[13] C. W. Gardiner and P. Zoller, *Quantum Noise*. Berlin, Germany: Springer-Verlag, 2000.

[14] I. Pérez-Arjona, E. Roldán, and G. J. de Valcárcel, "Quantum squeezing of optical dissipative structures," *Europhys. Lett.*, vol. 74, pp. 247–253, 2006.
[15] I. Pérez-Arjona, E. Roldán, and G. J. de Valcárcel, "Theory of quantum fluctuations of optical dissipative structures and its application to the squeezing properties of bright cavity solitons," *Phys. Rev. A*, vol. 75, pp. 063802-1–063802-15, 2006.
[16] J. Gea-Banacloche, N. Lu, L. M. Pedrotti, S. Prasad, M. O. Scully, and K. Wódkiewicz, "Treatment of the spectrum of squeezing based on the modes of the universe. I. Theory and a physical picture," *Phys. Rev. A*, vol. 41, pp. 369–380, 1990.
[17] E. Sharping, M. Fiorentino, P. Kumar, and R. S. Windeler, "Optical parametric oscillator based on four-wave mixing in microstructure fiber," *Opt. Lett.*, vol. 27, pp. 1675–1677, 2002.
[18] G. K. L. Wong, A. Y. H. Chen, S. G. Murdoch, R. Leonhardt, J. D. Harvey, N. Y. Joly, J. C. Knight, W. J. Wadsworth, and P. S. J. Russell, "Continuous-wave tunable optical parametric generation in a photonic-crystal fiber," *J. Opt. Soc. Amer. B*, vol. 22, pp. 2505–2511, 2005.
[19] T. J. Kippenberg, S. M. Spillane, and K. J. Vahala, "Kerr-nonlinearity optical parametric oscillation in an ultrahigh-Q toroid microcavity," *Phys. Rev. Lett.*, vol. 93, pp. 083904-1–083904-4, 2004.

Ferran V. Garcia-Ferrer was born in Gandia, Valencia, Spain, in 1966. He received the M.Sc. degree in physics in 1993 from the Universitat de València, Valencia, Spain, where he is currently working toward the Ph.D. degree at the Quantum and Nonlinear Optics Group.

Since 1994, he has been engaged in teaching physics and mathematics in high school. His current research interests include the quantum properties of light, and their application to quantum information science.

Carlos Navarrete-Benlloch was born in Valencia, Spain, in 1983. He received the M.Sc. degree in advanced physics in 2007 from the Universitat de València, Valencia, Spain, where he is currently working toward the Ph.D. degree at the Quantum and Nonlinear Optics group.

His current research interests include the quantum properties of light and cold atoms, and their application to quantum information science. For more information, see www.uv.es/nabencar.

Germán J. de Valcárcel was born in Valencia, Spain, in 1965. He received the Ph.D. degree in physics from the Universitat de València, Valencia, in 1993.

He is currently with the Universitat de València. His current research interests include the classical and quantum nonlinear dynamics of optical systems and the universality of dissipative structures.

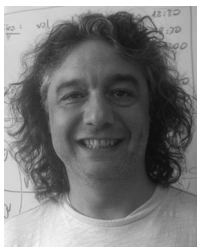

Eugenio Roldán was born in Valdepeñas, Spain, in 1965. He received the M.Sc. and Ph.D. degrees in physics in 1988 and 1993, respectively.

He is currently with the Universitat de València. He has been engaged in laser physics and quantum and semiclassical optics, with special interest in nonlinear dynamics, pattern formation, and squeezing. He has authored or coauthored around 80 papers on these subjects.